Locked-to-running transition in the two-dimensional underdamped driven Frenkel-Kontorova model

O. M. Braun,[1,*] M. V. Paliy,[1] J. Röder,[2] and A. R. Bishop[2]
[1]*Institute of Physics, National Ukrainian Academy of Sciences, UA-252022 Kiev, Ukraine*
[2]*Theoretical Division and CNLS, Los Alamos National Laboratory, Los Alamos, New Mexico 87545*
(Received 10 July 2000; published 27 February 2001)

We study the nonlinear dc response of a two-dimensional underdamped system of interacting atoms subject to an isotropic periodic external potential with triangular symmetry. We consider various values of the effective elastic constant of the system, two different atomic interaction potentials, and different concentrations of atoms. In the case of a closely packed layer, when its structure is commensurate with the substrate, there is a locked-to-running transition as a function of the driving force, whose mechanism depends on the effective elastic constant. For a low elastic constant, where the layer is weakly coupled, the transition is achieved via the creation of an avalanche of moving particles that leaves a depleted region in its wake. On increasing the effective elastic constant the depleted region becomes less marked and there is a crossover to a scenario in which an island of moving particles nucleates the transition. In the case of a partially filled atomic layer, several dynamical phase transitions between states with different atomic mobility are observed. The mobility of atoms as a function of the external force can vary nonmonotonically with increasing force. For the case of a small external damping, the system can be trapped at a large force in an immobile metastable state, thus demonstrating a ''fuse-safety device'' on an atomic scale.

DOI: 10.1103/PhysRevE.63.036129 PACS number(s): 05.70.Ln, 45.05.+x, 66.30.−h, 63.20.Ry

I. INTRODUCTION

The nonequilibrium dynamics of simple systems of interacting particles subject to an external periodic potential, damping, a thermal bath, and a driving force is a rich and interesting problem. As well as proving of theoretical interest, due to the array of unanswered questions, it has many important applications in fields such as dislocation theory [1], plastic flow of a solid [2], tribology [3], Josephson transmission lines, mass transport, and conductivity (e.g., see [4] and references therein).

The pioneering work on this subject, the case of one dimension and noninteracting atoms, was summarized in the monograph of Risken [5]. For a small applied force F, the total potential felt by a Brownian particle possesses an array of local minima. Hence, at zero temperature the mobility of the particles, defined as $B=\langle v\rangle/F$ (where v is the drift velocity of the atoms), vanishes and for low temperatures the mobility will be exponentially small. This is called the *locked* state. At some critical force F_c, the minima in the total potential vanish and the particle will slide over the corrugated total potential with a maximum mobility of $B=(m\eta)^{-1}$, where m is the mass of the Brownian particle and η is the viscous damping coefficient. This is known as the *running* or *sliding* state. In the underdamped case the system may possess a running solution even before the minima of the total potential vanish because the momentum of the particle can help it overcome the existing barriers.

The overdamped case of interacting atoms, the overdamped commensurate Frenkel-Kontorova (FK) model [6], is also well understood, thanks to work reducing the problem to a time-independent Schmoluchowsky equation [7]. As in the single particle case, hysteresis is present in the response of the system, but only at zero temperature.

A recent study of the one-dimensional (1D), *underdamped* FK model [8,9] has shown hysteresis in the locked to running transition even at *nonzero* temperature. The hysteresis was shown to result from a distinct difference in the mechanisms of the forward (locked-to-running) and backward (running-to-locked) transitions. The forward transition, seen on adiabatic increase of the driving force, is initiated by the instability of a fast moving kink (the topologically stable quasiparticle describing local compression of the one-dimensional chain) leading to an avalanche of kink-antikink pair production [8,10]. The kink becomes unstable upon reaching some critical velocity v_c which may be higher than the sound speed in the case of anharmonically interacting atoms [8]. The collision of the newly created kink and antikink initiates the growth of a domain of running atoms, which is characterized by a cosine density profile and expands with the sound speed [10]. This scenario is quite distinct from the reverse transition for adiabatically decreasing force, where intermediate steady states were observed to exist between the running and locked states [8].

One can define the coverage θ of such a FK system as the ratio of the number of atoms to the number of minima in the substrate potential. For commensurate coverages $\theta=1/m$, with m integer, it is first necessary to nucleate a kink-antikink pair via a thermal fluctuation. Then the instability of such topological kinks at high speeds will initiate the transition to the running state. When $\theta\neq 1/m$, residual (''geometrical'') kinks are already present in the undriven system and they become mobile before the transition to the running state [11,12]. In this case the transition has a multistep character. Additionally, if the interatomic interaction is anharmonic, the system passes through the nonuniform ''traffic jam'' steady state [9].

*Electronic address: obraun@iop.kiev.ua

The two-dimensional (2D) Frenkel-Kontorova model is obviously much more complicated than the 1D one. First, for 2D models we have no simple guide as we had in the 1D FK model, namely, the exactly integrable sine-Gordon equation. Practically all variants of the 2D model are not integrable even in the continuum limit. Second, even the ground state (g.s.) of the 2D model is often quite complicated. Depending on the substrate symmetry, interparticle potential, concentration, and temperature, the g.s. may be either crystalline (commensurate with the substrate), floating (incommensurate), liquid, or even totally chaotic as will be mentioned below in Sec. III. The g.s. problem was widely studied in the context of surface physics (e.g., see [13] and references therein). Third, the topological excitations of the 2D system, which, analogously to kinks in the 1D FK model, are responsible for the mobility, may be of different kinds; e.g., they may correspond to spatially localized excitations called ''crowdions'' (extra atoms inserted into the layer for the simplest $\theta=1$ structure) or to linear objects known as domain walls (DW's; sometimes the terms dislocation, discommensuration lines, or plane solitons are used). Moreover, the DW's themselves may be of different types, e.g., partial or total dislocations, edge or screw, etc.

The dynamics of the 2D FK model was studied mainly in the context of dislocation theory [1], when dislocation lines or a dislocation grid already preexist in the system. In the framework of the *scalar* 2D FK model, where the atoms are allowed to move in one dimension only, the DW motion is essentially the same as in the 1D FK model [14,15]. Only at high driving forces does the DW become unstable against spontaneous roughening, and the nucleation of additional wall-antiwall pairs behind the primary wall occurs. For a more realistic *vector* 2D FK model, where atoms can move in both x and y dimensions, there are only a few studies devoted to its dynamics. Notably, a 2D FK model with harmonic interactions between the atoms (the so-called ''spring and ball'' model) was studied in [16]. Here the emphasis was on dislocation generation and motion and the locked-to-running transition was not studied. Besides, in this model, only the interaction of nearest neighboring atoms was included. Thus the layer must keep its ordered state, and the model can be used for small mutual atomic displacements only.

A truly 2D FK model with the atoms able to move in all three dimensions, the atoms being subjected to the 3D external potential periodic in two dimensions and parabolic in the third dimension, was studied in [11,17] for an *anisotropic* rectangular substrate symmetry. The anisotropy of the system was established by the periodic part of the external potential, which was chosen as a set of ''channels'' with corrugated bottoms, oriented parallel to the direction of the applied force. In [17] the authors concentrated on studying the mobility of the system as a function of the atomic concentration θ, while in [11] the locked-to-running transition was considered. In the anisotropic 2D system the interaction between neighboring FK channels was found to lead only to minor changes of the behavior compared with the 1D system. Namely, when one of the channels passes to the running state, it carries the nearest neighboring channels into motion, so the straight river of running atoms grows until it occupies the whole system.

By contrast, investigations of the *isotropic* 2D underdamped *vector* FK system are very limited. In the context of tribology, Persson [18] studied a partially filled ($\theta\leqslant 0.5$) layer adsorbed on a substrate with square symmetry, and observed a hysteretic dynamical phase transition, similar to the $T=0$ one-particle case. However, there are still a number of open questions, in particular: (i) How does the transition begin for the commensurate $\theta=1$ system; does it start with the creation of a DW–anti-DW pair (dislocation loop) or with the emergence of a running island? (ii) How does the transition proceed after the nucleation event? (iii) How does the mechanism of the transition depend on the atomic concentration and on the layer structure? (iv) If a DW already preexists in the system, is its motion stable, and up to what velocity? (v) Does a spatially nonuniform ''traffic jam'' steady state appear during the transition?

The current study extends our understanding of the locked-to-running transition to the underdamped two-dimensional isotropic system. Here we shall consider a two-dimensional layer of particles with position vectors $\mathbf{u}=(u_x,u_y)$, subject to a periodic substrate potential. We use periodic boundary conditions in both spatial directions x and y. Although we do not intend either to develop a general theory of the locked-to-running transition in 2D systems or to consider some specific experimentally studied system, we have tried to choose a generic model which could exemplify and clarify the mechanism of the transition in the isotropic system. Namely, any two-dimensional periodic substrate potential can be constructed as a combination of four functions $s_{1,2}(x,y)=\sin(\mathbf{k}_{1,2}\cdot\mathbf{r})$ and $c_{1,2}(x,y)=\cos(\mathbf{k}_{1,2}\cdot\mathbf{r})$, where $\mathbf{k}_{1,2}$ are the corresponding reciprocal vectors. In the present work we chose the triangular lattice as typical of isotropic 2D systems, so the reciprocal vectors are $\mathbf{k}_1=(2\pi/a,-\pi/a_y)$ and $\mathbf{k}_2=(0,2\pi/a_y)$, where $a_y=a\sqrt{3}/2$. Similarly to the 1D FK model, where one takes $V_{\mathrm{sub}}(x)=\frac{1}{2}\varepsilon[1-\cos(2\pi x/a)]$, we will use the simplest symmetric combination $V_{\mathrm{sub}}(x,y)=\frac{1}{4}\varepsilon\{3-\cos(\mathbf{k}_1\cdot\mathbf{r})-\cos(\mathbf{k}_2\cdot\mathbf{r})-\cos[(\mathbf{k}_1+\mathbf{k}_2)\cdot\mathbf{r}]\}$ or

$$V_{\mathrm{sub}}(x,y)=\frac{1}{2}\varepsilon\left\{1-\cos\left(\frac{2\pi x}{a}\right)\cos\left(\frac{\pi y}{a_y}\right)+\frac{1}{2}\left[1-\cos\left(\frac{2\pi y}{a_y}\right)\right]\right\}. \tag{1}$$

The function (1) gives isotropic minima organized into a triangular lattice and separated by isotropic energy barriers of height ε, as shown in Fig. 1. The frequency of atomic vibration near the minima is also isotropic, $\omega_x=\omega_y=\omega_0\equiv(\varepsilon/2m)^{1/2}(2\pi/a)$. The function (1) has flat maxima of height ε (i.e., the same as the barriers) organized into a honeycomb lattice. Generally, introducing additional parameters one may construct a more complicated substrate potential, e.g., one with nonflat maxima. However, because the precise shape of the electronic density is not known for most surfaces, we prefer to use the simplest function (1). Similar

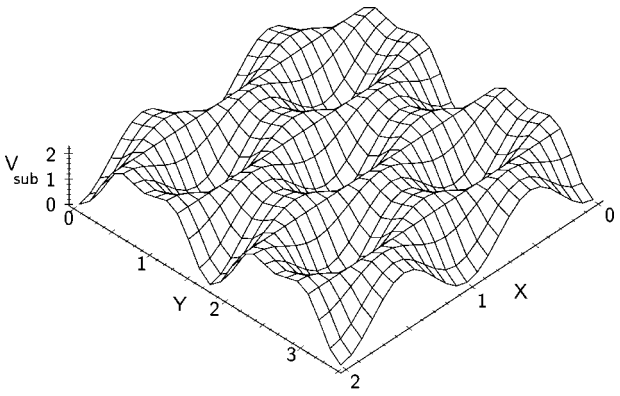

FIG. 1. The substrate potential with triangular symmetry, $V_{\rm sub}$, plotted for $\varepsilon=2$. The coordinates are scaled so that $X=x/a$ and $Y=y/a$.

forms of the substrate potential have been typically used in studies of atomic layers adsorbed on isotropic triangular and hexagonal substrates [13,19].

The atoms interact via a pairwise potential $V(r)$, where r is the interatomic separation. We have considered the cases of an exponential repulsion

$$V(r)=V_0\exp(-\gamma r), \tag{2}$$

with the choice $\gamma=a^{-1}$, and the Lennard-Jones (LJ) interaction

$$V(r)=V_0\left[\left(\frac{a}{r}\right)^{12}-2\left(\frac{a}{r}\right)^{6}\right]. \tag{3}$$

Notice that these two interactions are very different. The exponential case is purely repulsive with no minimum in the potential. This situation corresponds, in particular, to atoms chemically adsorbed on a metal surface, when, due to breaking of the translational symmetry in the direction normal to the surface, the atoms have a nonzero dipole moment which leads to their mutual repulsion [20]. For the LJ interaction there is both attraction and repulsion, with a minimum in the potential at the atomic separation $r=a$. When the atoms are closely packed and experience only the repulsive branch of the interaction as, for example, in the case of a lubricant film confined between two substrates, both potentials are qualitatively the same. But when the layer has expanded regions, where the interatomic separation exceeds the equilibrium distance $r=a$, the LJ potential may lead to first-order phase transitions. To avoid this complication, in most of our simulations we use simple exponential repulsion.

To characterize the system it is helpful to define the effective elastic constant $g_{\rm eff}=a^2V''(r_0)/2\pi^2\varepsilon$, where r_0 is the mean interatomic distance [4,21]. This single number gives an indication of the strength of the elastic constant of the layer of atoms relative to the strength of the substrate potential. A value of $g_{\rm eff}$ much smaller than 1 indicates a relatively weakly coupled layer, whereas a value much larger than 1 describes a stiff atomic layer compared with the substrate depth. Both large and small $g_{\rm eff}$ correspond to physically relevant systems. For a monolayer adsorbed on a surface, one is typically in the limit of low $g_{\rm eff}$ [20]. A lubricant layer between two blocks of material corresponds to the limit of large $g_{\rm eff}$. The fact that one has a block of material and not simply a free monolayer means that the layer immediately above the interface has a much larger effective elastic constant. Although the disturbances are limited to the layer of the block at the sliding interface, the other layers above help maintain the separation between the first layer and the lower block, reducing the effective substrate potential depth. Also, the other layers tend to lock the structure of the first layer, making it more rigid than a single monolayer.

We use a dimensionless system of units, where the atomic mass is $m=1$, the periodicity of the substrate potential is $a=2\pi$, and its height is $\varepsilon=2$, so that the characteristic frequency is $\omega_0=1$. It will also be helpful to define a time scale for the problem in terms of the oscillation period of a particle in the substrate potential, $\tau_s=2\pi$. One can also define a time scale in terms of the oscillation period of the particles in the layer, $\tau_0=\tau_s/\sqrt{g_{\rm eff}}$.

The equations of motion for the displacement vectors of the N atoms $\mathbf{u}_i(1\leqslant i\leqslant N)$ are given by

$$\ddot{v}_i+\eta\dot{v}_i+\frac{d}{dv_i}\left[\sum_{j(j\neq i)}V(|\mathbf{u}_i-\mathbf{u}_j|)+U_{\rm sub}(\mathbf{u}_i)\right]=F^v+F^v_{\rm rand}, \tag{4}$$

where $v=u_x$ or u_y, $F^v=F_x$ or F_y is the externally applied force, and $F^v_{\rm rand}$ is the random force required to equilibrate the system to a given temperature T. We chose the driving force to act only in the x direction, i.e., $F_x=F$, $F_y=0$. We typically used $\eta\sim0.1$, which is well underdamped, and chose T such that it was small compared to ε and the layer stiffness $V''(r_0)$ in order to obtain clearer pictures. Then, below the transition the mobility of the system is very small.

The numerical procedure for solving the equations was the same as used in previous reports [8,11]. First the atoms were thermalized at zero force; then the force was slowly (adiabatically) increased, allowing a time of several τ_s (or τ_0, if $\tau_0>\tau_s$) to equilibrate at each new value of the force. In this way the force was increased until one had moved through the transition. At each new value of the force the equilibrated configuration of positions and velocities was stored, allowing one to restart the simulation with a finer force step. Once the transition had been located for the system size and temperature the trajectories of the particles were examined carefully to allow the identification of the scenario for the transition.

The paper is organized as follows. First, in Sec. II we study the locked-to-running transition in the perfectly commensurate $\theta=1$ case, where the layer structure coincides with the substrate one. We show that the transition begins not with creation of a linear object such as a DW or dislocation loop, but with creation of a *localized* disturbed region, either a domain of running atoms for a stiff layer or a ''melted'' island for a weakly bound layer. These domains grow and finally overlap. In relatively small systems this leads to a *river* of running atoms. The width of the river then grows linearly with time until the whole system passes to the running state. For larger systems, the domains have longer to

develop before the periodic boundary conditions cause them to join up on themselves, and so the resulting structures are more complex. In Sec. III we present the results of an investigation of a specific but interesting case of the half-filled layer, $\theta=1/2$, when the system demonstrates new additional regimes such as a ''fuse safety'' scenario and a ''mirror switching'' steady state. Finally, Sec. IV concludes the paper with discussion of the results.

II. CLOSELY PACKED LAYER

First we consider the case of a closely packed atomic layer, $\theta=1$, when in the ground state the atomic layer has a triangular structure commensurate with the substrate. In the simulations we mostly studied a system of $N=N_xN_y=64\times64=4096$ atoms. To study system size dependence we looked at systems of up to $N=112\times112$ atoms, as well as systems with different aspect ratios.

Below, we analyze the locked-to-running transition for several values of $g_{\rm eff}$ for the two choices of the interatomic potential. The spectrum of the ideal triangular lattice is described by the functions $\omega_x^2(k)=\omega_g^2[3-2\cos(ak_x)-\cos(ak_x/2)\cos(a_yk_y)]$ and $\omega_y^2(k)=3\,\omega_g^2[1-\cos(ak_x/2)\cos(a_yk_y)]$, where $\omega_g=\sqrt{g_{\rm eff}}$ and $a_y=a\sqrt{3}/2$, so for the transverse wave propagating in the x direction (i.e., $k_y=0$) the group velocity is $v_T=\lim_{k_x\to0}\,d\omega_y(k)/dk_x=\sqrt{3}a\omega_g/2\sqrt{2}$, while for the longitudinal wave the group velocity is $v_L=\lim_{k_x\to0}\,d\omega_x(k)/dk_x=\sqrt{3}v_T$.

Because in the g.s. all atoms lie in substrate minima, the layer is strongly pinned. To initiate the motion, a topological defect (either a localized defect like crowdion or a dislocation loop) has to emerge first. The size of this defect must be of order $d\sim a\sqrt{g_{\rm eff}}$, so one could expect different scenarios for small and large values of $g_{\rm eff}$. Indeed, we found that around some threshold value of $g_{\rm eff}=g_1$ there is a crossover from one characteristic scenario to another in the early stages of the transition.

A. Stiff layer

In the regime $g_{\rm eff}\gg g_1$ the transition from the locked to running state is mediated by the formation of an island of moving atoms in a sea of essentially stationary particles. The size of the moving island grows quickly in the direction of the driving force and somewhat more slowly in the perpendicular direction. *Inside the island the atoms largely maintain their triangular structure* due to the stiffness of the atomic layer. Hence one sees areas of essentially perfect triangular lattice surrounded by a loop of partial dislocations. Due to the periodic boundary conditions, the island eventually joins up on itself. There is then a strip, oriented parallel to the driving force and bounded in the direction perpendicular to the driving force, in which particles move along the periodically continued system. Outside this strip the particles are immobile. We shall denote such a state as a *river*. The river then broadens perpendicular to the driving direction until all atoms are moving.

The evolution of this scenario is shown in a series of snapshots in Fig. 2. The same scenario was observed for both

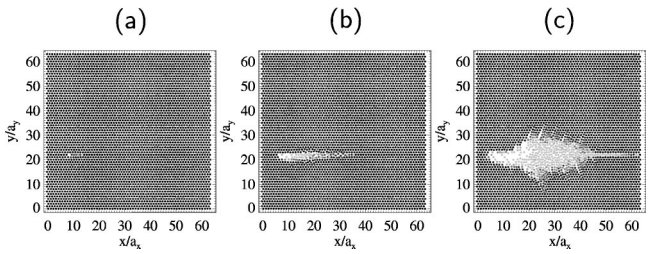

FIG. 2. Snapshots of the mechanism of the locked-to-running transition for the LJ interaction with $g_{\rm eff}=0.9$, $\eta=0.141$, $T=0.05$, and $F=0.9933$. The positions of the particles are indicated by circles. The x component of the particle velocity is shown in a grey scale by the color of the circle: black corresponding to zero velocity and the lightest grey to velocities over a certain velocity cutoff. Snapshots (b) and (c) are taken $0.27\,\tau_s$ and $0.54\,\tau_s$ after snapshot (a).

interactions. However, the value of g_1 above which the described scenario is observed is different for the LJ and exponential interactions. The LJ layer behaves more rigidly than the exponential case for the same value of $g_{\rm eff}$. We found that $0.1<g_1<1$ for the LJ case and $g_1\approx1$ for the exponential case.

The size of the island nucleated was found to increase with increasing $g_{\rm eff}$. As one increases $g_{\rm eff}$ further the characteristic nucleation island size increases towards the system size. For a very stiff layer of particles, $g_{\rm eff}>g_2$, the transition occurs via the whole system of atoms beginning to move. The value of g_2 naturally depends on the system size as well as on the details of $V_{\rm sub}(x,y)$ and $V(r)$. In particular, g_2 increases with N, so that one can mediate the transition with larger and larger islands by increasing the system size. For the same system size and temperature, the LJ interaction again proved stiffer than the exponential interaction, having a smaller value of g_2.

B. Weakly bound layer

For a weak interatomic interaction $g_{\rm eff}\ll g_1$, we found that the locked-to-running transition was mediated by the formation of an avalanche of moving particles leaving behind a depleted, low-density region. *The atoms in the disturbed region do not show a regular structure*, so we may speculate that the beginning of the locked-to-running transition is caused by the nucleation of a ''melted'' island. The exact scenario was slightly different for the two different interaction potentials.

First let us consider the exponential interaction. Snapshots of the system at three times during the transition are shown in Fig. 3 for the case of $g_{\rm eff}=0.1$. A thermal fluctuation starts a small number of particles moving in the direction of the driving force. This fluctuation persists long enough to locally destroy the triangular ordering of atoms and allows the atoms to escape the substrate minima. The moving atoms are accelerated by the driving force, leaving a depleted region behind them. The size of the disturbed region quickly grows in the direction of the driving force as the moving atoms impinge on stationary particles in front of them. Thermal fluctuations and the unbalanced repulsive interaction left by the atoms

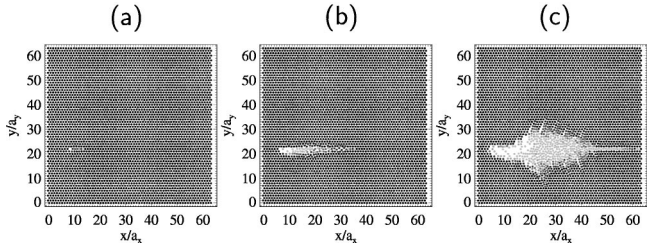

FIG. 3. Snapshots of the locked-to-running transition for the exponential interaction with $g_{\rm eff}=0.1$, $\eta=0.1$, $T=0.01$, and $F=0.94$. The positions of the particles are indicated by circles. The x component of the particle velocity is shown in a grey scale as in Fig. 2. Snapshots (b) and (c) are taken $6.3\,\tau_s$ and $12.3\,\tau_s$ after snapshot (a).

that have moved off their lattice sites cause stationary atoms adjacent to the depleted region to be easily set into motion. A dense region of atoms is created at the leading edge of the disturbance as the mobile particles are able to move faster than the leading edge can propagate. Mobile particles are therefore slowed down as they approach the leading edge, producing a dense region of slower particles, in much the same way as traffic slows down on approaching a hindrance on a road. We shall call this kind of situation a *traffic-jam* effect. The bulge at the leading edge of the disturbance grows both parallel and perpendicular to the driving force until the domain of moving atoms joins up on itself due to the periodic boundary conditions. The formation of the bulge is clearly visible in the two later snapshots of Fig. 3 (notice that in this particular simulation a second nucleation event also takes place).

The scenario observed for the LJ interaction is slightly different. Snapshots for the LJ interaction with $g_{\rm eff}=0.023$ are shown in Fig. 4. Again, a thermal fluctuation allows a small number of particles to start to move in the x direction. For the case shown in Fig. 4 this was four to five neighboring particles in the same $y=$const plane. The disturbed region quickly expands in the direction of the driving as in the case of the exponential interaction and again a depleted region is formed. In the LJ case the atoms in the wake of the disturbed region are set into motion by the attractive interaction between the particles at separations in excess of $r=a$. The

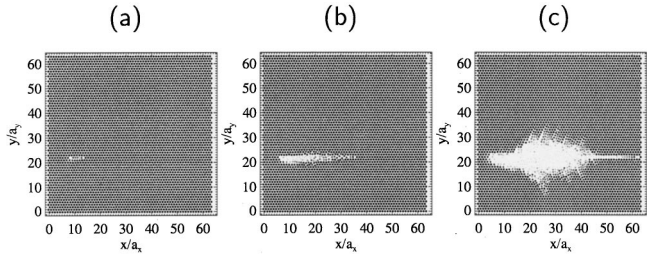

FIG. 4. Snapshots of the mechanism of the locked-to-running transition for the LJ interaction with $g_{\rm eff}=0.023$, $\eta=0.2$, $T=0.0025$, and $F=0.9901$. The positions of the particles are indicated by circles. The x component of the particle velocity is shown in a grey scale as in Fig. 2. Snapshots (b) and (c) are taken $0.45\,\tau_s$ and $1.1\,\tau_s$ after snapshot (a).

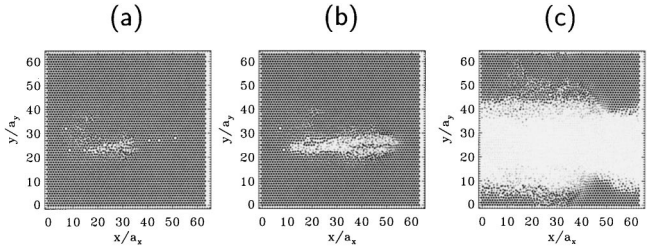

FIG. 5. Snapshots for the exponential interaction with one inserted atom for $g_{\rm eff}=0.3$, $\eta=0.1$, $T=0$, and $F=0.55$. The positions of the particles are indicated by circles. The x component of the particle velocity is shown in a grey scale as in Fig. 2. Snapshots (b) and (c) are taken $3.6\,\tau_s$ and $14.4\,\tau_s$ after snapshot (a).

effect of the moving particles creating a traffic-jam-like, denser region is different for the LJ interaction than for the exponential interaction. In the latter case a very dense region formed and produced a bulging out of the disturbed region. As can be seen in Fig. 4, for the LJ interaction the increased density causes the disturbed region to grow not only in the direction of the driving force, but also preferentially along the other two slip planes of the triangular lattice. The density at the leading edge of the disturbed region does not become as large as for the exponential interaction, and instead of bulging out the disturbed region develops ''barbs'' at angles $\pm\pi/3$ relative to the driving direction. At later times the disturbed region joins up with itself due to the periodic boundaries.

C. One extra atom

For the commensurate case described above, the first event in the forward transition is the creation of the disturbed region due to thermal fluctuations. The rate of this process is controlled by the Boltzmann factor $\exp(-\varepsilon_{\rm act}/T)$, where the activation energy is determined by the driving force, for example, $\varepsilon_{\rm act}\propto(1-F)^{1/2}$ in the $g_{\rm eff}\ll 1$ case. In the simulation we used low temperatures to reduce ''noise'' in the snapshots and, thus, we had to use forces very close to the maximum value, $F=1$. In order to check whether the scenario is different for lower forces, we also made simulations with one extra atom inserted into the commensurate structure. In the 1D FK model such a situation corresponds to one ''geometrical'' kink which easily moves through the lattice. In the isotropic 2D model studied in the present work, the configuration with one inserted atom surrounded by the ''distortion cloud'' (due to shifting of neighboring atoms around the inserted one) produces a localized configuration called a ''crowdion.'' Similarly to the 1D model, the crowdion moves much more easily than atoms of the background commensurate structure. At small F the crowdion performs directed random walks in the x direction, but sometimes it may also jump to the nearest neighboring x channel and push the atoms from their ideal positions. With increasing force, at some moment an additional crowdion-anticrowdion pair is created, and subsequently the avalanche starts to grow. The subsequent scenario was found to be the same as described above for the fully commensurate case and is shown in the snapshots of Fig. 5 for $g_{\rm eff}=0.3$. The critical force F_c when

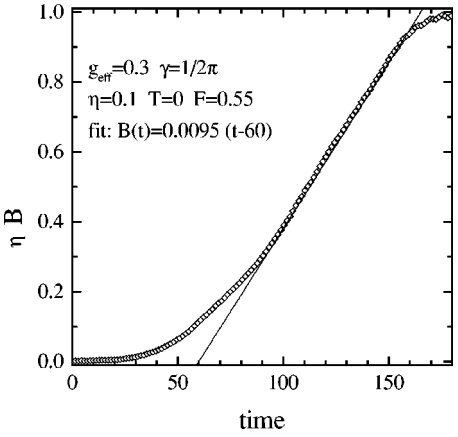

FIG. 6. The dependence of the mobility, B, on time for the locked-to-running transition for the initial configuration with one inserted atom in a 64×64 size system for $g_{\mathrm{eff}}=0.3$, $\eta=0.1$, $T=0$, and $F=0.55$.

the avalanche begins, however, is now much lower than in the fully commensurate case. For example, for the exponential interaction with $g_{\mathrm{eff}}=0.3$ we found $F_c\approx0.55$ at $T=0$.

Also, we checked the scenario of the locked-to-running transition for a high enough temperature, $T=1/3$, chosen so that the background structure is still commensurate, but the crowdion and also other atoms can move at small driving forces $F<0.3$. We found that the only qualitative difference from the $T=0$ case is that now the transition begins at a smaller force, $F_c\approx0.35$.

D. Later times

In all cases, the disturbed region eventually joins up on itself, due to the periodic boundary conditions. For relatively small square systems ($N\leqslant64\times64$) the moving domain did not have much opportunity to grow perpendicular to the driving force before joining with itself and so a *river* of moving particles was formed. The width of the river was found to grow approximately linearly with time, at a rate that decreased with increasing damping or temperature, until the whole system was in the running state. This scenario is quite general, because even in an infinite system, neighboring disturbed regions arising from thermal fluctuations will overlap with each other when they reach some critical size, as usual in percolation problems.

A typical snapshot of the atomic configuration during the river growth at $T=0$ is shown in Fig. 5(c) for the force $F_c=0.55$, where we used the initial configuration with one crowdion. In the middle of river the atoms move with almost the maximum velocity F_c/η and keep the ordered triangular structure. However, the boundary between the running and locked regions of the layer, which takes about ten atomic channels, is totally disordered. The rate of river growth, as seen from Fig. 6, may be approximated by a linear law $B(t)=\beta(t-t_0)$ with $\beta=0.0095$. From these data we can find the velocity of the river front as $v_R=N_y a_y \beta/2$. This gives $v_R\approx1.65$, which is approximately equal to $v_L/2$.

For larger square systems we see that the moving domain in fact grows considerably both perpendicular and parallel to the driving force. This can be seen in the snapshots of Fig. 7. At $T=0$ the leading, approximately semicircular, edge of the moving domain was found to both grow in diameter at a rate v and to propagate at speed c. Both v and c were found to be approximately equal to the longitudinal group speed v_L of the layer. As the moving domain then gains area by translational motion and growth we expect that the mobility should increase as t^2. The data for the 112×112 system are shown in Fig. 8 along with the quadratic fitted at early times.

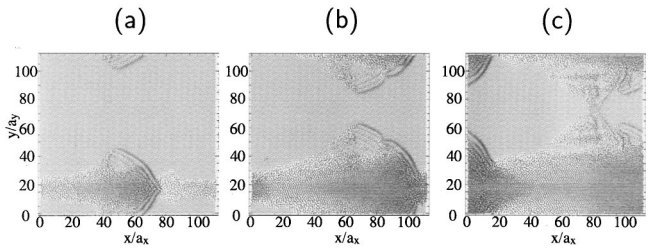

FIG. 7. Snapshots of the later stages of the locked-to-running transition for the 112×112 system, with the exponential interaction ($g_{\mathrm{eff}}=0.3$, $T=0$).

E. Backward transition

It has been observed for the 1D system [8] that spatially inhomogeneous stable states may exist when one decreases the driving force adiabatically from the running state. One might expect to find analogous stable states in the 2D system on the backward transition between running and locked states.

We have performed simulations of the running-to-locked transition (force decreasing) for the LJ interaction for the fully commensurate case and for three different values of g_{eff}.

(i) $g_{\mathrm{eff}}=10$. For the very stiff layer we show in Fig. 9 a plot of the mobility of the layer as a function of decreasing driving force. It is clear that stable states, with nonzero mobility, do exist between the running state (which exists for

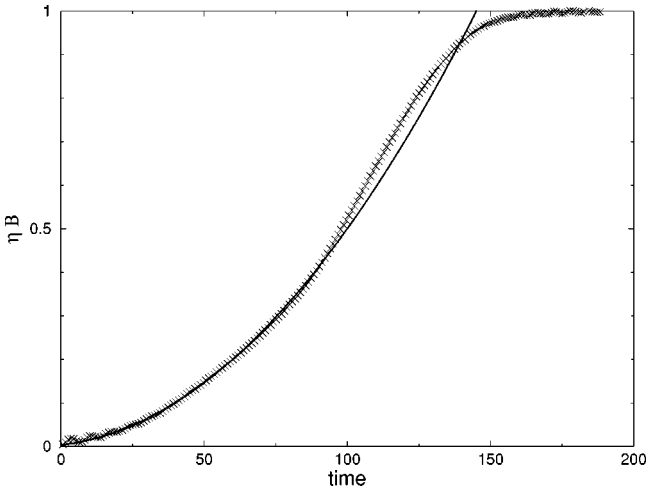

FIG. 8. The crosses show the mobility as a function of time for the locked-to-running transition for the 112×112 system, with the exponential interaction ($g_{\mathrm{eff}}=0.3$, $T=0$). The quadratic form fitted to the early time data is shown as the solid line.

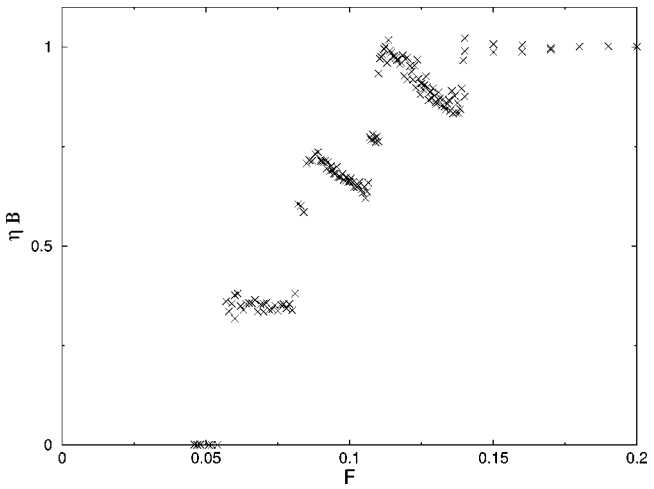

FIG. 9. Mobility as a function of decreasing driving force for the fully commensurate case, with LJ interaction, $g_{\rm eff}=10$. Intermediate stable states are clear between the running state $\eta B=1$ and the locked state $\eta B=0$.

$F>0.15$) and the locked state (which exists for $F<0.06$). For the system size studied ($N=64\times64$) we observed three large steps in the mobility curve, which correspond to spatially inhomogeneous states. These states are characterized on each step by the number of horizontal stripes of more mobile atoms present. The lowest mobility step was composed of states with one (or possibly a double) stripe of very mobile atoms, the middle step consisted of states with two (or two double) stripes, and the upper step corresponded to states with three (or three double) stripes.

On decreasing the force just below the stability of the running state ($F=0.15$), we first observed a state inhomogeneous in both spatial directions. Six small regions were observed where the velocity of the particles parallel to the driving force was clearly larger than average. We shall call each of these regions a *blob* and the state with n such regions an *n-blob* state. The observed six-blob state is shown in Fig. 10(a). Although reasonably long-lived ($\sim100\tau_s$) this six-blob state became unstable to a diagonal striped state, where the stripes of mobile atoms had a slope of 1/3. These states only appeared in a small range of F before the step with three horizontal stripes developed. Moving along the mobility

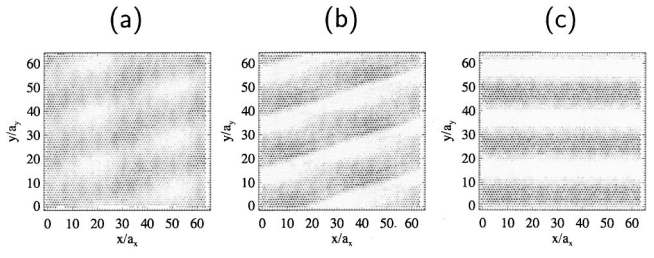

FIG. 10. Snapshots of (a) the six-blob state, (b) the three-diagonal-stripe state, and (c) the three-horizontal-stripe state for the LJ interaction ($g_{\rm eff}=10$) with fully commensurate coverage. The particles are color coded according to the x component of their velocity [black (slow) to light grey (fast)]. The blob state, although long lived, seems unstable to the diagonal-striped state.

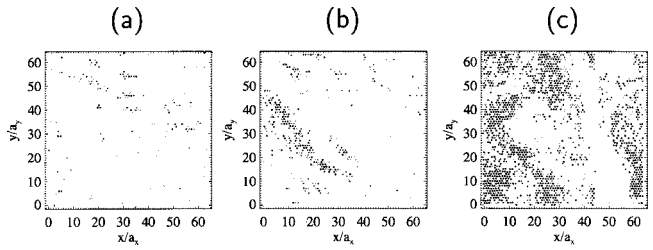

FIG. 11. Snapshots at various times through the running-to-locked transition for the LJ interaction ($g_{\rm eff}=1$) with fully commensurate coverage. The particles are color coded according to the x component of their velocity [black (slow) to light grey (fast)].

step, the width of the moving stripes of particles generally broadened. Examples of these three kinds of spatially inhomogeneous states observed are shown in Fig. 10. On continuing to decrease the driving force the mobility dropped sharply as a four-blob state was reached. Again this appeared to be unstable to a diagonal striped state, this time with a slope of 1/2. Then the middle step with states of two horizontal stripes was observed. Finally we noted a two-blob state, followed by a diagonal stripe with unit slope, and then a single horizontal stripe of more mobile atoms.

We expect that it may be possible to predict the locations of the steps in the mobility curve by developing a linear stability analysis about the running state, as can be done for the 1D system, using the approach of Ref. [22]. However, the analysis is severely complicated by the complexity of the 2D phonon spectrum and the nonorthogonal lattice vectors of the triangular lattice. As with the 1D system, one expects that increasing the system size would increase the number of steps present on the mobility curve. It would seem, from the emergence of the blob states, that the linear stability analysis selects a particular unstable wavelength of the 2D system. The nonlinearity appears to force the system to saturate into a stable striped state, rather than maintaining a state periodic in both x and y directions.

(ii) $g_{\rm eff}=1$. For this value of effective elastic constant no stable intermediate states were observed. However, one could observe the transient behavior between running and locked states. At first one could observe small regions of stationary or slow moving particles in a sea of mobile ones. Initially these regions appeared completely randomly positioned; however, they soon began to cluster until the entire system was in the locked state. Although the system studied was fully commensurate, the final state of the simulations was not completely locked, due to the presence of vacancies and corresponding crowdions. These would have eventually disappeared to leave the completely locked, low-temperature state; however, the time scale for the mobile crowdions to diffuse perpendicular to the driving force and annihilate with the pinned vacancies was very long. Snapshots showing the progression through the transition are shown in Fig. 11.

(iii) $g_{\rm eff}=0.023$. When the layer is weakly coupled compared with the substrate strength, we observed that the locked-to-running transition occurred via a different scenario. Namely, a disordered band of particles formed parallel to the driving force, which contained the slow moving particles. Apart from a few vacancies, the region outside the

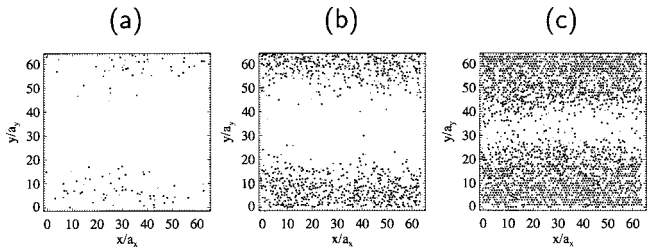

FIG. 12. Snapshots at various times through the running-to-locked transition for the LJ interaction ($g_{\rm eff}=0.023$) with fully commensurate coverage. The particles are color coded according to the x component of their velocity [black (slow) to light gray (fast)].

band was made up of ordered highly mobile particles. The band broadened and the density of slow particles increased, until the disordered region spanned the whole system, at which point the slow particles were mainly clustered in a band parallel to the driving direction. The width of the band of slow particles then grew to span the whole system. Again, generally one observed a few vacancies and crowdions in the final state of the simulation that had not had time to anneal out of the system. The scenario of the transition is illustrated in the series of snapshots of Fig. 12.

III. HALF-FILLED LAYER

Now let us consider again the commensurate atomic layer but with the concentration $\theta=1/2$. Recall that in the 1D FK model this case is exactly the same as the $\theta=1$ one. For the isotropic 2D model the situation, however, differs drastically.

In this simulation we studied the case of exponential repulsion only, in order to avoid formation of closely packed islands. The exponent γ was chosen larger than that in the simulations described above, $\gamma=0.37$, and the effective elastic constant was chosen to be small, $g_{\rm eff}=0.15$, because such values are more typical for adsorbed layers [20]. Besides, we also allowed the atoms to move in the direction normal to the surface, using the 3D substrate potential $V_{\rm sub}^{(3D)}(x,y,z)=V_{\rm sub}(x,y)+\frac{1}{2}\omega_z z^2$ with $\omega_z=1.67$. These parameters are the same as used in the study of the anisotropic rectangular 2D FK model [11,12], so we can compare the behavior of the anisotropic and isotropic models. The temperature was chosen to be very small as above, $T=0.0022$.

A. Ground-state configuration

To find the minimum energy configuration, we started with different typical initial configurations, allowed the system to relax at $F=0$ and $T\to 0$, and then compared the energies of the final configurations [23]. Although this technique cannot guarantee the true ground state, we believe that, in combination with qualitative arguments, it can be used to find the ground state of the system.

There are two plausible atomic arrangements in the neighboring rows for the concentration $\theta_0=1/2$. The first is the $p(2\times1)$ structure, and the second corresponds to atoms arranged in a zigzaglike fashion, so that the configuration has the ''distorted'' $c(2\times2)$ structure shown in Fig. 13(a). In

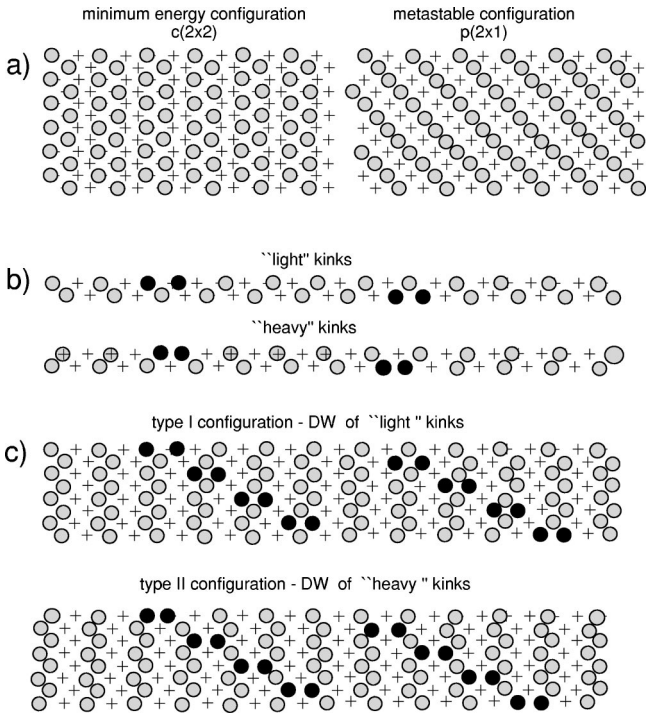

FIG. 13. Atomic structure at the $\theta_0=1/2$ background coverage. Atoms are denoted with gray circles, atoms in the kink regions are denoted with black circles, and minima of the external potential are denoted with crosses. (a) $c(2\times2)$ structure (minimum energy configuration) and $p(2\times1)$ structure (metastable configuration); (b) two types of kinks, ''light'' kinks and ''heavy'' kinks; (c) configuration with the domain walls of ''light'' kinks at $\theta=21/40$.

the framework of a lattice-gas model, where the atoms can be placed only at the minima of the substrate potential, the most energetically favorable structure is $p(2\times1)$. However, for the continuous model under study here the situation is inverted: for the chosen set of parameters the $c(2\times2)$ structure provides the absolute minimum of energy. Indeed, in the continuous model the atoms in the ''zigzags'' of $c(2\times2)$ structure are slightly shifted from the positions of the substrate minima, thus lowering the energy of repulsion between them, and the decreasing of the interaction energy exceeds the increase of energy due to atomic displacements from the substrate minima. Note that this relaxed $c(2\times2)$ structure may more easily be translated along the substrate; i.e., it experiences a lowered effective barrier due to shifts of some atoms.

Now let us consider possible structures of kinks and domain walls on the background of the $c(2\times2)$ structure. The $c(2\times2)$ structure for the triangular substrate is 12-fold degenerate: there are three rotational variants of the structure, each of them has additionally two translational types, and each translational type has also two mirror-image variants. Therefore, when the concentration slightly deviates from the background value $\theta_0=1/2$, there exist a number of different types of DW's which link different types of the $c(2\times2)$ domains. For concreteness, in the simulation we chose the $c(2\times2)$ domain which is symmetrical relative to the driving force, as shown in Fig. 13(a), and inserted an incommensu-

rability in the direction along the force. The two possible minimal incommensurabilities are shown in Fig. 13(b). In the first configuration, the center of a kink in one row is placed in front of the occupied site in the nearest neighboring row, and for the second configuration the kink center opposes an empty site in the neighboring row. The kinks of the first kind may be named the ''light'' kinks, because, as we explicitly checked, they have a smaller energy than the kinks of the second kind (the ''heavy'' kinks).

For kinks constructed on the background of a $\theta_0<1$ structure, the kinks in the nearest neighboring x rows always attract each other according to $V_{\rm atr}(x)\propto|x|$ and, therefore, they have to be organized into linear domain walls. [The DW lines should be tilted with respect to the y direction due to short-range kink-kink repulsion $V_{\rm rep}(x)\propto\exp(-\gamma x)$, which arises from the repulsion of extra atoms contained in the kinks.] The attraction $V_{\rm atr}(x)$ emerges because of an energetically unfavorable atomic arrangement between the kinks [17]. However, for the case of the $c(2\times2)$ structure, the amplitude of attraction is lower than that for the rectangular substrate [17], because now the kinks are inserted not into each x row but into every second row, and the atomic arrangement in the rows lying between the rows with kinks is similar to that outside the kinks [see Fig. 13(b)]. Note that the domain wall can contain kinks of one type only (either ''light'' or ''heavy'' kinks), providing that the commensurate structure between the pair of walls is the minimum energy $c(2\times2)$ structure, and not the energetically unfavorable $p(2\times1)$ structure. Analogously to single kinks, we will call such domain walls ''light'' and ''heavy'' walls.

As the initial state for the study of nonlinear mobility, we used the configuration with ''light'' domain walls, although the evolution of the configuration with ''heavy'' walls will be briefly commented on as well. The chosen initial configuration is shown in Fig. 13(c). In the simulation we used $N=40\times20=420$ atoms, so the coverage is $\theta=21/40$, and the regions of the $c(2\times2)$ structure are separated by ''light'' DW's with average spacing of $10a$.

B. Nonlinear mobility

The dependences of the mobility B on the adiabatically changing force F are shown in Fig. 14 for two values of the friction constant, $\eta=0.15$ and $\eta=0.35$. One can see several intermediate regimes between the locked state $B=0$ and the running state $B=1$. First, at $F=F_k\approx0.18$, the mobility sharply increases, and with further increase of force the mobility remains approximately constant, $B\approx0.1$. Figure 15(a) demonstrates a typical atomic configuration at this plateau. One can see that the atoms perform motion only in the regions of DW's, while atoms in the body of the $c(2\times2)$ domain are immobile. Thus, this plateau corresponds to the running state of ''light'' DW's, and the threshold F_k is to be interpreted as the Peierls-Nabarro force, at which the barrier for translation of DW's is eliminated. Interestingly, *the running domain walls are stable* and, moreover, the initially tilted DW's line up perpendicular to the applied force during the motion.

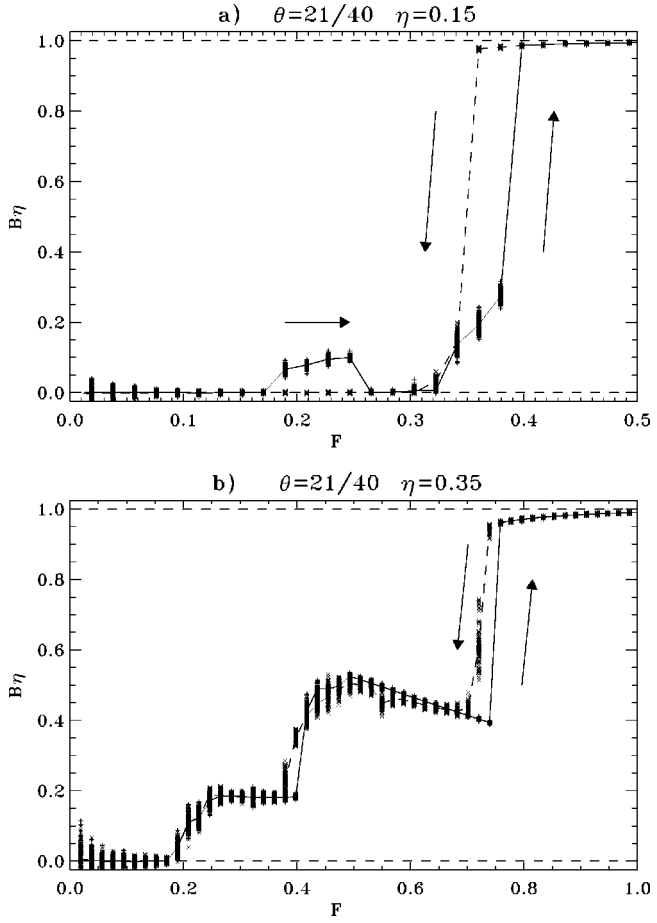

FIG. 14. The mobility B versus the external force F for $\theta=21/40$ at (a) the low friction $\eta=0.15$ and (b) the high friction $\eta=0.35$.

With increasing applied force, the velocity of running DW's increases, but the subsequent scenario depends on the value of the friction coefficient. For a low friction constant $\eta=0.15$, at a certain critical force $F=F_d\approx0.26$ the domain walls become unstable. This results in disordering of the whole system, which loses the $c(2\times2)$ structure [as seen in the snapshot of Fig. 15(b)] and becomes a disordered state. Because a concerted atomic motion (running DW's) is no longer possible in this disordered state, the system comes back to the *locked* state with $B=0$. Note that this locked state is *metastable*—it has a higher energy than the initial ordered configuration. One may recall in this connection the ''frustration'' problem for a triangular lattice-gas (or Ising) model at the coverage $\theta_0=1/2$ (e.g., see [24] and references therein). Namely, if the repulsion of atoms in the lattice-gas model is restricted to nearest neighbors only, the ground state at $\theta_0=1/2$ is infinitely degenerate and therefore disordered. In the continuous model, as well as for a larger range of the interatomic interaction, an ordered ground state does exist [the $c(2\times2)$ structure in our case], but it may be surrounded by metastable-disordered states with only slightly higher energies. Thus, with increasing force, when the system energy increases due to kinetic energy of running DW's, the system may be trapped in such a metastable state. A nonzero mobility in the system appears again at $F>F_m$

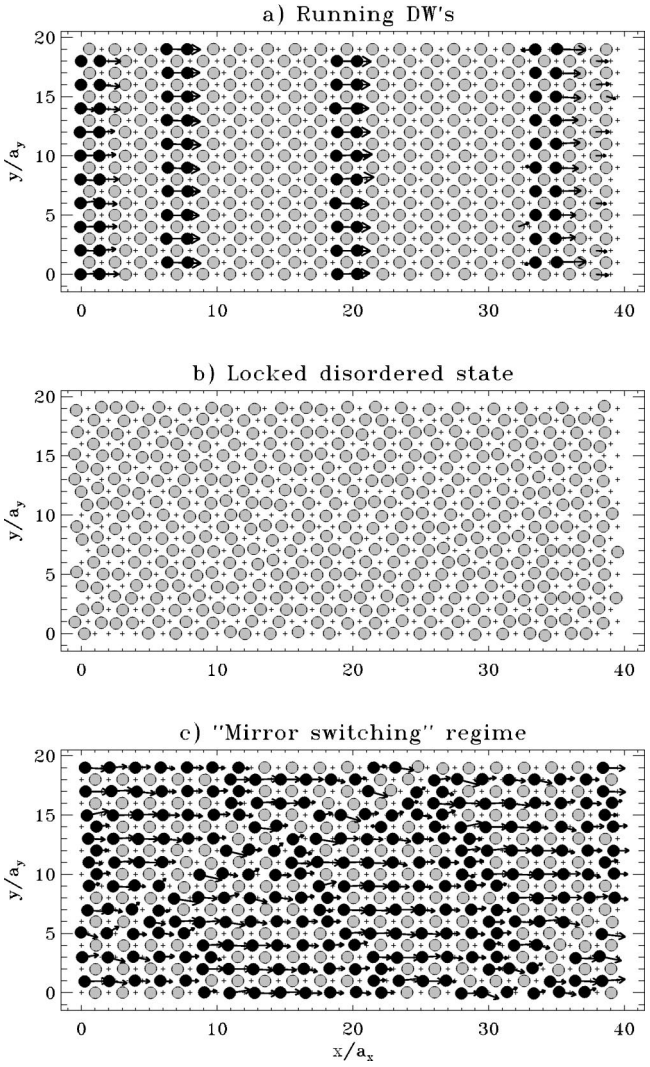

FIG. 15. Atomic patterns at the intermediate stages of $B(F)$ dependences plotted in Fig. 14: (a) regime of running DW's, (b) locked disordered state, and (c) ''mirror switching'' regime. Immobile atoms are denoted with gray circles; running atoms and atoms in the kink regions are denoted with black circles; arrows indicate the direction of atomic motion.

≈ 0.32, and at $F=F_f \approx 0.4$ the system evolves to the totally running state with $B=1$.

On the other hand, for a higher friction $\eta=0.35$, the drift velocity of domain walls is much lower than for the low η case, and the ordered running-DW steady state survives until the second critical force $F=F_m \approx 0.4$, so that the intermediate locked state with $B=0$ does not appear. Now there are two intermediate plateaus in the $B(F)$ dependence, one at $F_k<F<F_m$ with the mobility $B\approx 0.2$ corresponding to DW motion and the second plateau in the interval of forces $F_m<F<F_f$ (where $F_f \approx 0.75$) with mobility $B\approx 0.5$. The atomic motion at the second intermediate stage is illustrated in Fig. 15(c). Here the atoms move not only in the regions of domain walls, but in the body of the $c(2\times 2)$ structure. At an instant of time, only *half* of the atoms in a single $c(2\times 2)$ domain can move, namely, the atoms situated in the center of the $c(2\times 2)$ unit cell. For instance, all atoms belonging to even rows in Fig. 15(c) can move to the neighboring empty sites inside their cells, thus changing the symmetry of the given $c(2\times 2)$ domain to its mirror image. Then, another sublattice (the atoms in odd rows) can move in the same manner, thus reverting the structure to the previous symmetry. Therefore, this regime corresponds to a periodic change of the $c(2\times 2)$ domain symmetry between its two mirror images, as illustrated in Fig. 15(c), so it may be called the ''mirror switching'' regime. Because only half of the atoms are moving at any instant of time, the mobility is $B\eta \approx 0.5$. The ''mirror switching'' regime exists also for the truly commensurate $\theta_0=1/2$ case, when the initial configuration does not contain residual kinks.

C. Dynamical phase diagram

The results of simulations are summarized in the phase diagram (F,η) shown in Fig. 16, where we plot the forward critical forces F_k, F_d, F_m, F_f, and also the critical force F_b for the backward transition, as functions of the friction η. Let us first consider the forward transition. At low frictions, $\eta<0.1$, with increasing of the force the system is transferred directly from the locked state to the totally running state, and there are no steady-state intermediate regimes. In more detail, at $F_k \approx 0.18$ there is a transient process, when the ''light'' domain walls are destroyed as soon as they start to move, and the system goes to a disordered metastable state. As this disordered state may be different for different frictions, this explains why the forward critical force F_f depends on friction in this region, despite the fact that the preceding state is immobile.

The interval of higher frictions, $0.1<\eta<0.2$, is characterized by nonmonotonic change of the mobility with increasing force. For this friction interval, there are all three subsequent intermediate stages described above: the regime of running DW's, the disordered immobile state, and the ''mirror switching'' regime. The critical force F_d for destruction of ''light'' DW's increases approximately linearly with η, which evidences that the critical quantity for determining stability of the domain walls is their drift velocity $\langle v_c \rangle \propto F_d/\eta$. This behavior is in agreement with the study of quasi-1D FK system [12], where it has been found that the drift velocity of kinks defines the dynamical phase transitions between the intermediate stages.

At higher frictions $\eta>0.2$, the mobility again varies monotonically with force, because the critical drift velocity v_c for running domain walls cannot now be reached, and the DW's are stable up to the critical force F_m, where the transition to the ''mirror switching'' regime takes place. The dependence of the forward critical force F_f on the friction η is also very close to a simple linear form $F_f \propto \eta$.

Consider now the backward transition. Note that in Fig. 16 we showed only the first critical force F_b, which corresponds to the first sharp drop of the mobility from the running $B=1$ state to a state with a lower mobility $B<1$, although at high frictions the backward transition has a multistep character, as is shown in Fig. 14. Namely, one can distinguish three friction regions differing by the scenario of the backward transition. At low frictions $\eta<0.1$, the system

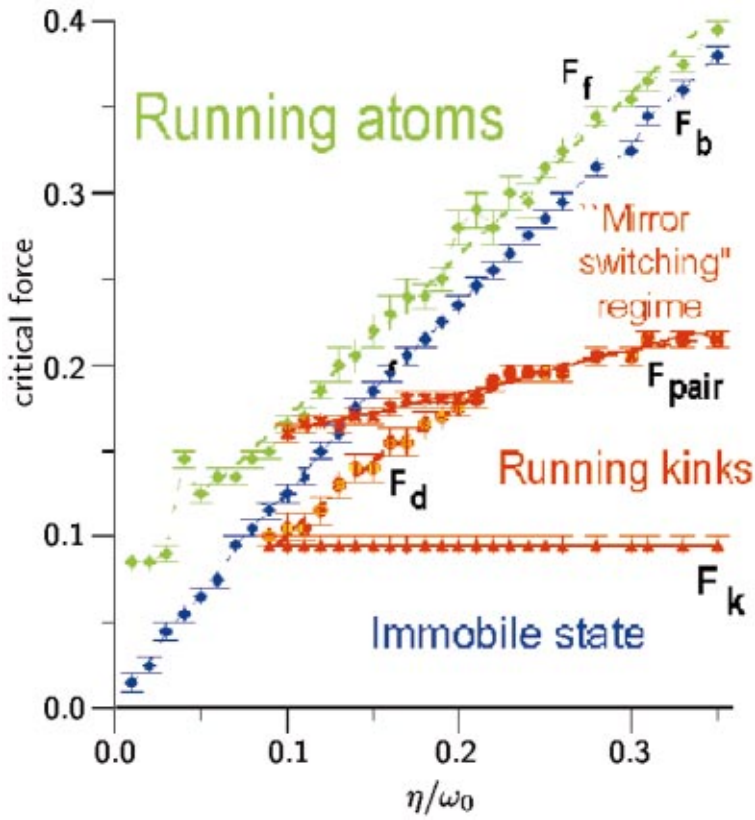

FIG. 16. (Color) Dynamical phase diagram in the (F,η) plane for the triangular FK model at $\theta=21/40$ coverage.

goes directly from the $B=1$ state to the $B=0$ state. At higher frictions $0.1<\eta<0.2$, the ''mirror switching'' regime exists during the backward transition, while the regime of running ''light'' DW's is absent, because this transition proceeds at a critical force slightly lower than F_m. Finally, at $\eta>0.2$ the condition for the stable motion of ''light'' DW's is fulfilled at $F<F_m$, and the regime of running DW's may exist. In fact, we observed that at not too high frictions $\eta \approx 0.2$–0.25 the system may either choose the ''running DW'' attractor during the backward transition or it may go directly to the immobile state. But at higher frictions $\eta > 0.25$, the system always shows the last plateau of the running ''light'' DW's at the backward transition, and only becomes completely immobile at $F<F_k$.

Finally, let us describe the evolution of an initial configuration with ''heavy'' DW's. The only difference in the $B(F)$ dependence at the forward transition for the ''heavy'' DW's is that the running-DW regime does not exist. The Peierls-Nabarro barrier for the ''heavy'' kinks is too high, and the system goes directly to the ''mirror switching'' regime. However, the scenario of the backward transition does not depend on the initial configuration. At high friction, if one starts from the configuration with ''heavy'' DW's, during the backward transition the system always chooses the attractor of the running ''light'' DW's.

IV. CONCLUSION

We have reported a detailed numerical study of the locked-to-running transition for the isotropic two-dimensional Frenkel-Kontorova model with triangular symmetry of the substrate potential and driven by a dc external force in the underdamped limit.

For the commensurate $\theta=1$ structure we found a crossover between two different scenarios around $g_{\rm eff}=g_1$. When the atomic layer is rather weakly coupled compared to the substrate potential depth the transition occurs via the formation of a depleted region and an avalanche of moving particles results. For larger values of $g_{\rm eff}$ the transition is mediated by the formation of islands of moving particles, which maintain an essentially triangular structure. The details of the scenario for small $g_{\rm eff}$ were found to be slightly different for the two interactions studied. In the case of the LJ interaction the influence of the moving particles was seen to spread rapidly down the slip planes of the lattice and the maximum particle density observed was relatively low. For the exponential interaction the observed densities were much higher and no indication of the lattice planes was observed in the shape of the disturbed region at high forces.

For large $g_{\rm eff}$ the mechanism of the transition was found to be independent of the interaction used. One may expect that this is generally true for all interaction potentials, as in the case of the rigid layer the particles can only make small deviations from their relative positions and thus are insensitive to many of the details of the interaction. In the weakly coupled layer, however, depleted and denser regions form, so a wider range of interparticle separations occur, causing differences between various potentials to be more apparent. The density differences observed are easily explained by the rapidly increasing strength of the LJ interaction at small separations, compared with the exponential repulsion which re-

mains finite at zero separation. In all cases the LJ interaction behaved more stiffly than the exponential interaction for the same value of g_{eff}.

For the totally commensurate case, the first event in the forward transition is the creation of the disturbed region due to thermal fluctuations. The rate of this process is controlled by the Boltzmann factor $\exp(-\varepsilon_{\mathrm{act}}/T)$, where the activation energy is determined by the driving force, $\varepsilon_{\mathrm{act}} \propto (1-f)^{1/2}$. However, if an extra atom preexists in the lattice, it performs directed random walks at small f, while at large forces the scenario was found to be the same as for the fully commensurate case. The critical force f_c when the avalanche begins, however, is now much lower than in the commensurate case.

A study of the reverse running-to-locked transition indicates hysteresis and the existence of other stable states, as was found in the one-dimensional case [8]. The intermediate stable states between running and locked states were formed by stripes (either diagonal with slope $1/m$, where m is an integer, or parallel to the driving force) of mobile atoms.

In the case of the half-filled layer $\theta = 0.5$, for a certain range of frictions the mobility can vary *nonmonotonically* with force. After the intermediate regime of running domain walls, the system can be trapped in a metastable disordered immobile state due to destruction of the running domain walls when they reach a critical velocity. Such a behavior occurs due to the existence of additional degrees of freedom in the 2D FK model and does not exist in the standard FK model. A nonmonotonic $B(F)$ dependence may also appear in other generalized versions of the FK model, if there are metastable states with energies close to the ground state, in particular, in the FK model with a transverse degree of freedom [25].

For the $\theta = 0.5$ case we also found a new stage, the *''mirror switching''* regime, which emerges due to a complex structure of the ground-state configuration [namely, the nonempty centered unit cell for the $c(2\times 2)$ structure]. Thus, the symmetry of the substrate (which determines the ground-state structure) can drastically affect the scenario of the nonlinear response of the two-dimensional atomic layer to the external force.

It should be possible to observe the scenarios for both g_{eff} large and small in physically relevant systems. For a monolayer adsorbed on a surface one is typically in the limit of low g_{eff}. So, on forcing, a depleted, low-density region should be observed during the transition. The adsorbed films may also be prepared with any coverage $\theta < 1$, so the ''fuse safety'' scenario and the ''mirror switching'' regimes could be observed in these systems.

Island formation has already been observed in large-scale molecular dynamics tribology simulations [26]. Here the simulations are of a two-dimensional interface between two blocks of material, which is characterized by a large effective elastic constant. A comparison of the molecular dynamics data with results from a 2D FK model with parameters matched to the molecular dynamics system shows similar island formation features [27].

Finally, we mention an important role of defects in the kinetics of the locked-to-running transition. The defects may serve as centers for nucleation of moving islands at the beginning of the transition or as sources for creation of new dislocations thus increasing the mobility of the whole layer. On the other hand, the DW's may be pinned by the defects thus decreasing the mobility. These processes have been widely considered in the context of dislocation theory [1], surface diffusion [28], and in studies of the magnetic flux lines in high-temperature superconducting films [29]. All these studies are restricted, however, to either the 1D FK model or to the scalar 2D model, and usually correspond to the overdamped limit. The investigation of the role of defects in the underdamped driven 2D-isotropic FK model certainly deserves a separate detailed study.

ACKNOWLEDGMENTS

We gratefully acknowledge helpful discussions with T. Dauxois, J. E. Hammerberg, B. L. Holian, R. P. Mikulla, and M. Peyrard. This research is supported in part by the U.S. DOE under Contract No. W-7405-ENG-36 and NATO Grant No. HTECH.LG.971372. The work of M.P. was also partially supported by the Hong Kong Research Grant Council and Hong Kong Baptist University Faculty research grants.

[1] J. P. Hirth and J. Lothe, *Theory of Dislocations* (Wiley, New York, 1982).
[2] F. R. N. Nabarro, Philos. Mag. A **75**, 703 (1997).
[3] B. N. J. Persson, *Sliding Friction: Physical Principles and Applications* (Springer-Verlag, Berlin, 1998); Surf. Sci. Rep. **33**, 83 (1999).
[4] O. M. Braun and Yu. S. Kivshar, Phys. Rep. **306**, 1 (1998).
[5] H. Risken, *The Fokker-Planck Equation* (Springer, Berlin, 1984).
[6] Ya. Frenkel and T. Kontorova, Phys. Z. Sowjetunion **13**, 1 (1938).
[7] S. E. Trullinger *et al.*, Phys. Rev. Lett. **40**, 206 (1978); **40**, 1603 (1978); M. Büttiker and R. Landauer, Phys. Rev. A **23**, 1397 (1981); M. Büttiker and T. Christen, Phys. Rev. Lett. **75**, 1895 (1995).
[8] O. M. Braun, A. R. Bishop, and J. Röder, Phys. Rev. Lett. **79**, 3692 (1997).
[9] O. M. Bran, B. Hu, A. Filippov, and A. Zeltser, Phys. Rev. E **58**, 1311 (1998).
[10] O. M. Braun, B. Hu, and A. Zeltser, Phys. Rev. E **62**, 4235 (2000).
[11] O. M. Braun, T. Dauxois, M. V. Pally, and M. Peyrard, Phys. Rev. Lett. **78**, 1295 (1997); Phys. Rev. E **55**, 3598 (1997).
[12] M. Paliy, O. Braun, T. Dauxois, and B. Hu, Phys. Rev. E **56**, 4025 (1997); O. M. Braun, T. Dauxois, M. V. Paliy, M. Peyrard, and B. Hu, Physica D **123**, 357 (1998).
[13] I. F. Lyuksyutov, A. G. Naumovets, and V. L. Pokrovsky, *Two-Dimensional Crystals* (Academic, Boston, 1992).
[14] J. Pouget, S. Aubry, A. R. Bishop, and P. S. Lomdahl, Phys. Rev. B **39**, 9500 (1989).

[15] E. B. Kolomeisky, T. Curcic, and J. P. Straley, Phys. Rev. Lett. **75**, 1775 (1995).
[16] P. S. Lomdahl and D. J. Srolovitz, Phys. Rev. Lett. **57**, 2702 (1986); D. J. Srolovitz and P. S. Lomdahl, Physica D **23**, 402 (1986).
[17] O. M. Braun, T. Dauxois, M. V. Paliy, and M. Peyrard, Phys. Rev. B **54**, 321 (1996).
[18] B. N. J. Persson, Phys. Rev. Lett. **71**, 1212 (1993); Phys. Rev. B **48**, 18 140 (1993).
[19] R. G. Caflisch, A. N. Berker, and M. Kardar, Phys. Rev. B **31**, 4527 (1985); K. Kern and G. Comsa, *Kinetics of Ordering and Growth at Surfaces*, edited by M. G. Lagally (Plenum Press, New York, 1990).
[20] O. M. Braun and V. K. Medvedev, Usp. Fiz. Nauk **157**, 631 (1989) [Sov. Phys. Usp. **32**, 328 (1989)].
[21] S. Aubry, Physica D **7**, 240 (1983).
[22] J. C. Ariyasu and A. R. Bishop, Phys. Rev. B **35**, 3207 (1987).
[23] O. M. Braun and M. Peyrard, Phys. Rev. B **51**, 17 158 (1995).
[24] D. P. Landau, Phys. Rev. B **27**, 5604 (1983); A. Pelizzola, Phys. Rev. E **54**, 5885 (1996).
[25] O. Braun, M. Paliy, and B. Hu, Phys. Rev. Lett. **83**, 5206 (1999).
[26] R. P. Mikulla, J. E. Hammerberg, P. S. Lomdahl, and B. L. Holian, in *Fundamentals of Nanoindentation and Nanotribology*, edited by N. R. Moody *et al.*, Mater. Res. Soc. Symp. Proc. No. 522 (Materials Research Society, Pittsburgh, 1998), p. 385.
[27] R. P. Mikulla, J. Röder, and J. E. Hammerberg (unpublished).
[28] I. F. Lyuksyutov and V. L. Pokrovsky, Pis'ma Zh. Eksp. Teor. Fiz. **33**, 343 (1981) [JETP Lett. **33**, 326 (1981)].
[29] G. Blatter *et al.*, Rev. Mod. Phys. **66**, 1125 (1994); D. R. Nelson and V. M. Vinokur, Phys. Rev. B **48**, 13 060 (1993).